SBI

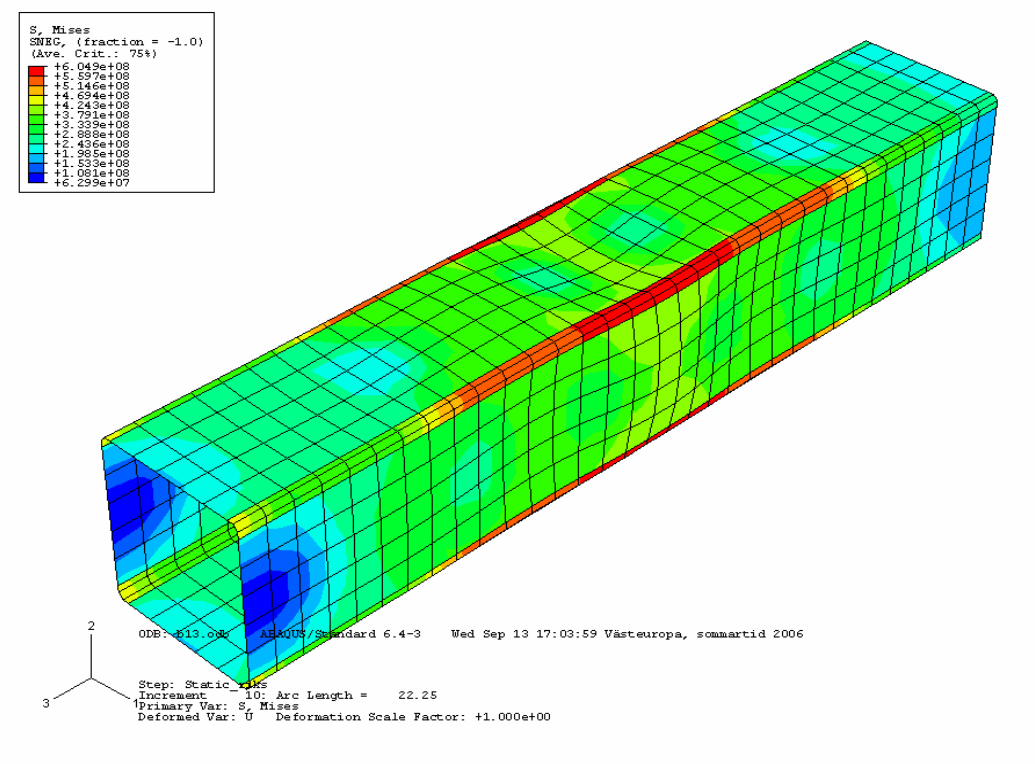

Stainless Steel in Fire

RFS-CR-04048

WP 3 – Analysis and design guidance on Class 4 members in fire
Final report

Björn Uppfeldt

The Swedish Institute of Steel Construction, SBI

10-04-2007

1. Executive summary

The use of stainless steel in buidings is small but rising. Mainly due to the low maintenance costs, favourable corrosion resistance and aesthetic appearance. Recent research projects have shown that stainless steel also performs better than carbon steel at elevated temperatures. The improved behaviour is mainly explained by the enhanced material properties and a favourable temperature dependent relationship between strength and stiffness that makes stainless steel less prone to buckling in fire.

The objective of this work package is to establish and validate a new simple design model for Class 4 stainless steel box columns in fire. The proposed design model is verified through parametric studies performed with the finite element software Abaqus and the FE-model used for the parametric studies is validated towards Class 4 stub column tests at both ambient and elevated temperatures.

The failure mode of Class 4 box columns is a combination of local and flexural buckling. The importance of taking the temperature dependent relationship between strength and stiffness into account is clearly seen in the results from the parametric study.

The proposed design model is fully compatible with EN 1993-1-1 (2005) and its capability to predict failure loads at different steel temperatures is compared to the design model in Design Manual for Structural Stainless Steel (2006). All design models are then compared to the results of the parametric study. The results show an improvement from a mean of 0,96 and COV=0,17 to a mean of 0,99 with a COV=0,12.

2. Contents

3. Introduction

The use of stainless steel in buildings is small but rising. Mainly due to the low maintenance costs, favourable corrosion resistance and aesthetic appearance. Several recent RFCS projects and published results in Karlström (2004), Ng & Gardner (2006), have shown that stainless steel performs better than carbon steel at elevated temperatures. The improved behaviour is mainly explained by the enhanced material properties and a favourable relationship between strength and stiffness that makes stainless steel less prone to buckling in fire. For flexural buckling this behaviour is taken into account in EN 1993-1-2 (2005) and Design Manual for Structural Stainless Steel (2006) but not for local buckling. This makes the Eurocode treatment inconsistent and it leads to conservative results especially for slender cross-sections.

In the following the work undertaken in order to collect enough data to propose a new design model is presented as well as the design model it self.

The work is a result of the RFCS project Stainless Steel in Fire. Contract No. RFS-CR-04048.

4. Objective

The purpose of this work is to provide simple design rules for Class 4 stainless steel box columns in fire. The design model was verified through parametric studies performed with the finite element software Abaqus. The FE-model used for the parametric studies was validated towards stub column tests made within the project by VTT, Finland at both ambient and elevated temperatures.

5. Experimental Work

The experimental work within this work package was performed by VTT and is presented in detail in Ala-Outinen (2007). A brief summary follows.

Four stub columns of cold rolled stainless steel, $\overline{\lambda} < 0,1$, with cross-section Class 4 at ambient temperature and six similar columns at elevated temperature were tested. The material used in the columns was EN 1.4301 and the material properties were determined from longitudinal tensile coupon tests of the flat faces of the columns. The geometry of the columns as well as the local imperfections were measured. Fully restrained ends were achieved in experiments. The cross-sections are made from hot-rolled sheets that are formed to circular sections and welded. The circular sections are then cold roll-formed to square sections. The welds are located in the middle of one side of the cross-section.

The results are presented in Table 5.1 and 5.2.

Table 5.1 ***Results from tests at the ambient temperature.***

No. specimen	Cross-section	Length (mm)	Failure load (kN)
A13	200x200x5	900	1129
A16	200x200x5	900	1118
B13	150x150x3	900	398
B16	150x150x3	900	393

Table 5.2 ***Results from tests at elevated temperatures***

No. specimen	Cross-section	Length (mm)	Load (kN)	Load level	Temperature at failure (C°)
A11	200x200x5	900	694	0,62	609
A12	200x200x5	900	567	0,50	685
A15	200x200x5	900	463	0,41	764
B11	150x150x3	900	203	0,51	676
B14	150x150x3	900	165	0,42	720
B15	150x150x3	900	248	0,63	588

6. Numerical Analysis

6.1 Evaluation of experimental results with FE-analysis

6.1.1 Geometry

General

In order to prove the validity of the FE-model the numerical results are compared to results from experiments.

The test set up is described in Ala-Outinen (2007).

Elements

Type

A general-purpose shell element within Abaqus/Standard called S4R is chosen for all simulations. S4R is a 4-node, quadrilateral, stress/displacement element with reduced integration and six degrees of freedom. By general purpose is meant that the element can be used for both thick shells where transverse shear flexibility is important and for thin shells where transverse shear is negligible. When the thickness of the shell increases S4R uses thick shell theory and when the thickness decreases S4R becomes a discrete Kirchoff thin shell element. For homogenous shells transverse shear flexibility is negligible when the thickness is less than about 1/15 of a characteristic length on the surface of the shell, such as the distance between supports or the wavelength of a significant eigenmode, ABAQUS/Standard manual (2001). Although the tested columns are far from thick and computational time could have been saved with a thin element such as S9R5 or similar a general-purpose element was chosen in order not to introduce any limitations for the parametric study.

Size

To confirm a chosen element size a sensitivity study is a useful tool. Different element sizes were analysed with respect to computational time and accuracy. The results of the sensitivity study are presented in Table 6.1.

Table 6.1 ***Results of sensitivity study on column B13 according to Table 5.1***

Element type	Element size	Element size relative to side length of the column	N_u from non linear analysis	CPU time
S4R	0,025 m	~b/6	396 kN	127 s
S4R	0,0125 m	~b/12	387 kN	474 s
S4R	0,006125 m	~b/24	385 kN	2227 s

The S4R element with an element size of b/6 is chosen due to the relatively small difference in results (~3%) compared to the large difference in CPU time.

6.1.2 Material properties at room temperature

General

For the flat faces of the columns the ultimate and proof strength used for the validation of the FE-model were obtained from the tensile tests performed within the project by VTT, Ala-Outinen (2007). However, due to the production process of the columns (cold roll-forming) the corner regions have an increased effective yield strength from cold forming. Therefore the cross-sections are divided into parts with different ultimate and proof strength in the corner regions compared to the flat faces, Figure 6.1. Gardner & Nethercot (2004) have found that extending the corner properties to 2*t* beyond the curved portions of the cross section in FE models gives the best agreement with test results.

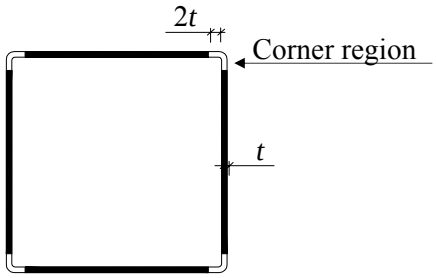

Figure 6.1 ***Section***

FE modelling

In Abaqus/Standard material data is given as true stresses and logarithmic strains. This means that all measured and calculated stresses and strains have to be converted before used in the FE-software. The Abaqus/Standard manual (2001) gives a simple model for this, Equation 6.1 and Equation 6.2.

$$\sigma_{\text{true}} = \sigma_{\text{nom}}(1+\varepsilon_{\text{nom}}) \tag{6.1}$$

$$\varepsilon_{\text{ln}}^{\text{pl}} = \ln(1+\varepsilon_{\text{nom}}) - \frac{\sigma_{\text{true}}}{E} \tag{6.2}$$

The nominal values are taken from the approximated stress-strain curves, see below, to calculate the material input used in Abaqus/Standard.

Material properties

The elastic modulus and the Poisson's ratio are not affected by cold forming and hence it is taken as E=200 000 MPa and ν=0,3 for the whole cross section.

Flat faces

The stress-strain relationship was taken as an average of all tensile coupon tests performed on each column, Figure 6.2.

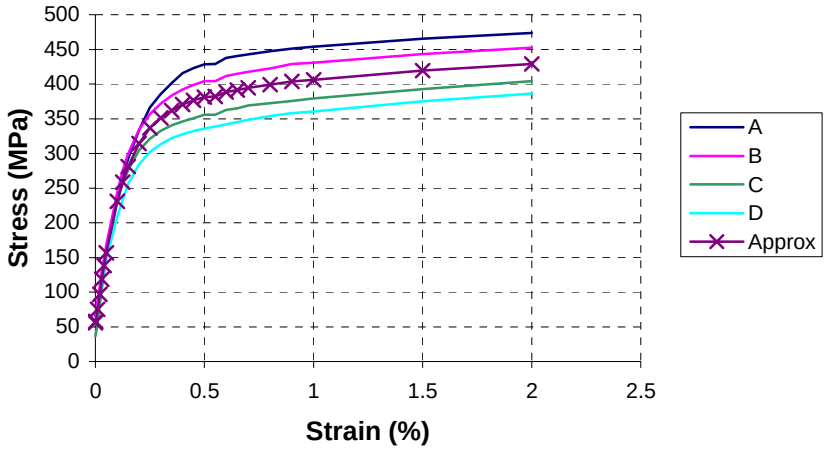

Figure 6.2 ***The stress-strain curve for the different cross-sections is taken as the average from the tensile coupon tests. The stress-strain curves for cross-section 150x150x3 are shown.***

The 0,2% proof strength, $f_{0.2}$, and the ultimate strength, f_u, for the columns were taken as the mean values from tensile tests of the faces. Two tests were performed on two different sides of each cross-section. For virgin material the 0,2% proof strength, $f_{0.2,v}$, and the ultimate strength, $f_{u,v}$, the values were taken from the steel mill certificates, Table 6.2.

Table 6.2 ***Material properties for the different sections***

Section	$f_{0.2}$ (MPa)	f_u (MPa)	$f_{0.2,v}$ (MPa)	$f_{u,v}$ (MPa)
RHS 150x150x3	363	654	336	645
RHS 200x200x5	314	623	289	621

Corner regions
Since no tensile tests were carried out on the material in the corner regions the corner 0,2% proof strength has to be estimated. Ashraf et al. (2005) have made a comparison of the available methods and suggests to use the following equation.

$$f_{0.2,c} = \frac{1.881 f_{0.2,v}}{\left(\frac{r_i}{t}\right)^{0.194}} \tag{6.3}$$

where: r_i is the inner corner radius and t is the cross-section thickness.

According to Ashraf et al. (2005) the ultimate corner strength can be predicted in accordance with Equation 6.4.

$$\sigma_{u,c} = 0,75\sigma_{0,2,c}\left(\frac{\sigma_{u,v}}{\sigma_{0,2,v}}\right) \tag{6.4}$$

The material properties derived from Equation 6.3 and 6.4 are presented in Table 6.3 below.

Table 6.3 ***Material properties of the corner regions for the different sections***

Section	$f_{0.2}$ (MPa)	f_u (MPa)
RHS 150x150x3	536	776
RHS 200x200x5	510	823

The mathematical stress-strain model in EN 1993-1-2 (2005), Figure. 6.3, was used to get the stress-strain relationship from the derived ultimate and proof strength, Figure 6.4.

Strain range	Stress σ	Tangent modulus E_t
$\varepsilon \le \varepsilon_{c,\theta}$	$\frac{E \cdot \varepsilon}{1 + a \cdot \varepsilon^b}$	$\frac{E(1 + a \cdot \varepsilon^b - a \cdot b \cdot \varepsilon^b)}{(1 + a \cdot \varepsilon^b)^2}$
$\varepsilon_{c,\theta} < \varepsilon \le \varepsilon_{u,\theta}$	$f_{0.2p,\theta} - e + (d/c)\sqrt{c^2 - (\varepsilon_{u,\theta} - \varepsilon)^2}$	$\frac{d + (\varepsilon_{u,\theta} - \varepsilon)}{c\sqrt{c^2 - (\varepsilon_{u,\theta} - \varepsilon)^2}}$
Parameters	$\varepsilon_{c,\theta} = f_{0.2p,\theta}/E_{a,\theta} + 0.002$	
Functions	$a = \frac{E_{a,\theta}\varepsilon_{c,\theta} - f_{0.2p,\theta}}{f_{0.2p,\theta}\varepsilon_{c,\theta}^{\ b}}$	$b = \frac{(1 - \varepsilon_{c,\theta}E_{ct,\theta}/f_{0.2p,\theta})E_{a,\theta}\varepsilon_{c,\theta}}{(E_{a,\theta}\varepsilon_{c,\theta}/f_{0.2p,\theta} - 1)f_{0.2p,\theta}}$
	$c^2 = (\varepsilon_{u,\theta} - \varepsilon_{c,\theta})\left(\varepsilon_{u,\theta} - \varepsilon_{c,\theta} + \frac{e}{E_{ct,\theta}}\right)$	$d^2 = e(\varepsilon_{u,\theta} - \varepsilon_{c,\theta})E_{ct,\theta} + e^2$
	$e = \frac{(f_{u,\theta} - f_{0.2p,\theta})^2}{(\varepsilon_{u,\theta} - \varepsilon_{c,\theta})E_{ct,\theta} - 2(f_{u,\theta} - f_{0.2p,\theta})}$	

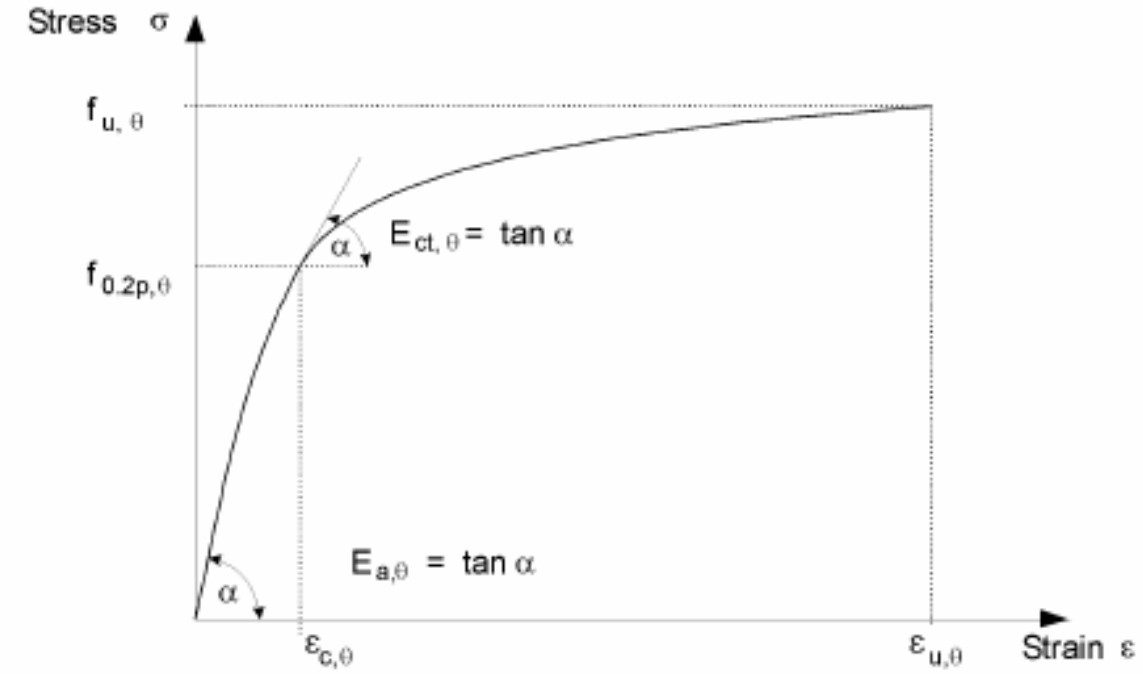

Key:

$f_{u,\theta}$	is	tensile strength;
$f_{0.2p,\theta}$	is	the proof strength at 0.2% plastic strain;
$E_{a,\theta}$	is	the slope of the linear elastic range;
$E_{ct,\theta}$	is	the slope at proof strength;
$\varepsilon_{c,\theta}$	is	the total strain at proof strength;
$\varepsilon_{u,\theta}$	is	the ultimate strain.

Figure 6.3 ***Mathematical stress-strain model in EN 1993-1-2 (2005)***

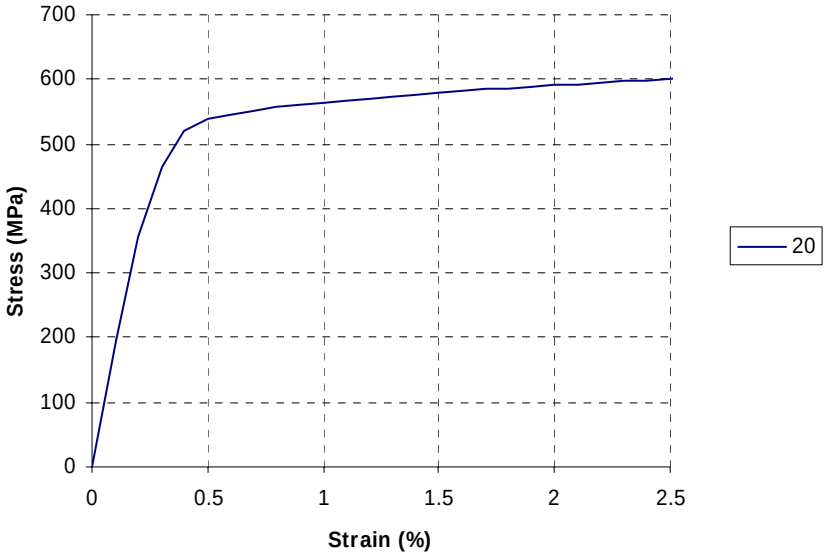

Figure 6.4 ***Stress-strain curve for the cold formed corner regions, cross-section 150x150x3***

6.1.3 Material properties at elevated temperatures

General

The material properties are changing with temperature and since no tensile coupon tests have been performed on the columns in fire the stress-strain relationship at elevated temperatures are based on the material model used for the cold-formed regions at room temperature. To describe the change of the material properties with temperature reduction factors are introduced in the Eurocodes. The reduction factors needed to derive the stress-strain curves are defined as:

- Slope of linear elastic range, relative to slope at 20 °C: $k_{E,\theta} = E_{a,\theta} / E_a$
- 0,2 % proof strength, relative to strength at 20 °C: $k_{0,2p,\theta} = f_{0,2p,\theta} / f_{0,2p}$
- Slope at proof strength, relative to slope at 20 °C $k_{Ect,\theta} = E_{ct,\theta} / E_{ct}$

FE modelling

When using temperature dependent thermal elongation coefficients they have to be converted to total elongation before being defined in Abaqus/Standard. The Abaqus/Standard Manual (2001) gives expressions for the conversion, Equation 6.5 and 6.6.

$$\alpha_n = \varepsilon_n^{th} / \left(\theta_n - \theta_{n-1}\right) \tag{6.5}$$

$$\varepsilon_n^{th} = \varepsilon_{n-1}^{th} + \alpha_n' \left(\theta_n - \theta_{n-1}\right) \tag{6.6}$$

where α'_n is a series of constant values between temperatures θ_{n-1} and θ_n.

Material properties

To model the temperature-induced expansion the equation for thermal elongation in Design Manual for Structural Stainless Steel (2006) is used, Equation 6.7, and then converted to total elongation according to the above.

$$\Delta l / l = (16 + 4,79 \cdot 10^{-3} \cdot \theta_a - 1,243 \cdot 10^{-6} \cdot \theta_a^{\,2}) \cdot (\theta_a - 20) \cdot 10^{-6} \qquad (6.7)$$

where:
l is the length at 20°C
Δl is the temperature-induced expansion
θ_a is the steel temperature (°C)

Flat faces
The stress-strain relationship was derived from the mathematical material model in Figure 6.3 based on the material properties at room temperature and reduction factors according to Design Manual for Structural Stainless Steel (2006), Table 6.4. The stress-strain curves for different temperatures are shown in Figure 6.5.

Table 6.4 ***Reduction Factors for the flat faces of the cross-section***

Temperature (°C)	$k_{0.2,p,\theta}$	$k_{u,\theta}$	$k_{E,\theta}$	$k_{Ect,\theta}$
20	1.00	1.00	1.00	0.11
100	0.82	0.87	0.96	0.05
200	0.68	0.77	0.92	0.02
300	0.64	0.73	0.88	0.02
400	0.60	0.72	0.84	0.02
500	0.54	0.67	0.80	0.02
600	0.49	0.58	0.76	0.02
700	0.40	0.43	0.71	0.02
800	0.27	0.27	0.63	0.02
900	0.14	0.15	0.45	0.02

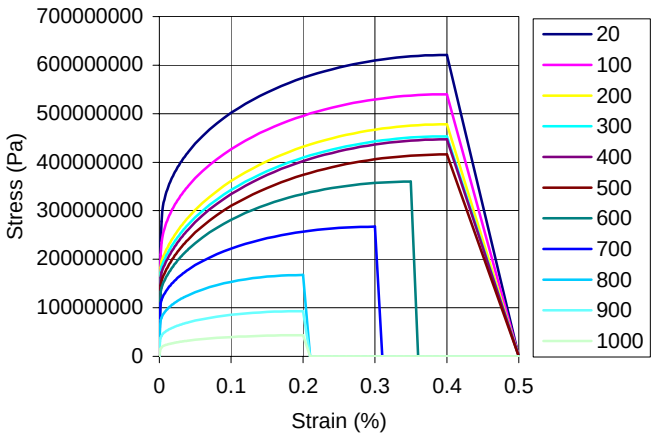

Figure 6.5 ***Stress-strain curves at elevated temperatures for column 200x200x5***

Corner regions
The Eurocodes give no specific reduction factors for cold formed stainless steel. It has been shown by Zhao & Blanguernon (2004) that the reduction factor for the annealed grade 1.4571 in EN 1993-1-2 (2005) overestimates the strength values of cold worked material for temperatures above 700 °C and underestimates the values when the temperature is below 700 °C, Table 6.5. The same behaviour is also recognized for other stainless steel grades tested.

In Finland, VTT has tested cold-formed EN 1.4301 in fire, Ala-Outinen (1996). The tests show that the same also applies for the cold-formed material in the corner regions of a cold-formed RHS column. In Table 6.6 the reduction factors derived from VTTs test results for both the virgin sheet and

the corner regions are compared to the reduction factors for EN 1.4301 in EN 1993-1-2 (2005). As seen in the table VTTs reduction factors for the virgin sheet is a bit higher, less than 10%, than the factors in EN 1993-1-2 (2005). However the difference between the reduction factors for the cold-formed material and the virgin sheet are significant and consequently not using these factors will lead to conservative results below 700 °C. Table 6.7 shows all reduction factors used in the FE-model for the cold-formed corner regions.

Table 6.4 ***Comparison of the reduction factors for cold worked (C850) and annealed EN 1.4531***

Temperature (°C)	*EN 1.4531 C850 Zhao (2xxx)* $k_{0.2,p,\theta,c}$	*EN 1.4531 Annealed EN 1993-1-2 (2005)* $k_{0.2,p,\theta,c}$
20	1.00	1.00
100	0.96	0.89
200	0.95	0.83
300	0.92	0.77
400	0.89	0.72
500	0.83	0.69
600	0.81	0.66
700	0.60	0.59
800	0.35	0.50
900	0.10	0.28

Table 6.5 ***Comparison of the reduction factors for cold formed and annealed EN 1.4301***

Temperature (°C)	*EN 1.4301 cold-formed Ala-Outinen (1996)* $k_{0.2,p,\theta,c}$	*EN 1.4301 annealed Ala-Outinen (1996)* $k_{0.2,p,\theta}$	*EN 1.4301 annealed EN 1993-1-2 (2005)* $k_{0.2,p,\theta}$
20	1.00	1.00	1.00
100	0.91	0.83	0.82
200	0.88	0.74	0.68
300	0.83	0.69	0.64
400	0.80	0.66	0.60
500	0.70	0.59	0.54
600	0.64	0.52	0.49
700	0.42	0.43	0.40
800	0.28	0.30	0.27
900	0.10	0.18	0.14

Table 6.6 ***Reduction factors used in the FE-model***

Temperature (°C)	$k_{0.2,p,\theta,c}$	$k_{u,\theta,c}$	$k_{E,\theta,c}$	$k_{Ect,\theta,c}$
20	1.00	1.00	1.00	0.050
100	0.91	0.86	0.96	0.050
200	0.88	0.79	0.92	0.050
300	0.83	0.76	0.88	0.050
400	0.80	0.74	0.84	0.050
500	0.70	0.64	0.80	0.046
600	0.64	0.57	0.76	0.036
700	0.42	0.40	0.71	0.036
800	0.28	0.27	0.63	0.036
900	0.10	0.14	0.45	0.036

6.1.4 Geometrical imperfections

The two types of geometrical imperfections that have to be considered are global imperfections and local imperfections.

One way to model geometrical imperfections in finite element software is by using a sinusoidal shape from an eigenvalue buckling analysis and set the amplitude to the relevant imperfection. The analysis gives a sinusoidal shape corresponding to an instability mode and by using the shape of the lowest eigenvalue the imperfections modelled will be conservative.

Another way to model imperfections is by moving the nodes manually into a shape corresponding to measured imperfections. This alternative is rather easy for modelling global imperfections but for local imperfections the use of an eigenvalue buckling analysis is the simpler and faster option. Consequently the eigenvalue buckling analysis is used for the local imperfections and for the global imperfections the nodes are moved manually into a half sine wave on the middle half of the columns.

To evaluate the influence of geometrical imperfections a sensitivity analysis was performed, where the magnitudes of both the local and global imperfections were varied. For the eigenvalue analysis the subspace iteration method in Abaqus/Standard was used. When the imperfections were set a load-deflection (Riks) analysis was performed to get the compression resistance of the column. The Riks method uses the load magnitude as an additional unknown and to measure the progress of the solution the "arc length", *l*, is used along the static equilibrium path in load-displacement space, Abaqus/Standard Manual (2001). The load is proportional and a new load is calculated for each increment and to solve the nonlinear equilibrium equations Abaqus/Standard uses Newton's method. Table 6.8 presents the results of sensitivity analysis and Figure 6.6 and 6.7 show the shape of the initial imperfections for local and global imperfections, respectively.

Table 6.7 ***Compression resistance of column B13***

Local imperfection	Global imperfection			
	L/1000	(-)L/1000	L/500	None
b/100	383 kN	383 kN		382 kN
b/200	401 kN	401 kN	398 kN	401 kN
(-)b/200	401 kN	401 kN		401 kN
None	489 kN	488 kN	486 kN	610 kN

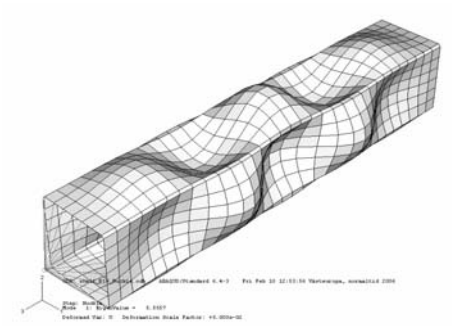

Figure 6.6 ***Shape of local imperfections***

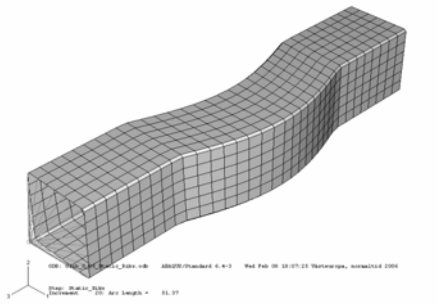

Figure 6.7 ***Shape of global imperfections***

It can be seen from the small differences in compression resistance that the magnitudes of the global imperfections are negligible and that the magnitudes of the local imperfections have small influence on the compression resistance as long as it is larger than zero.
For the modelling of the tested columns the measured local imperfections were used, Ala-Outinen (2007), and no global imperfections were introduced.

6.1.5 Residual stresses

Gardner & Nethercot (2004) came to the conclusion that residual stresses causes a small reduction in stiffness but have little influence of the overall behaviour or ultimate load carrying capacity for stub columns.

No residual stresses are introduced in the modelling of the tested columns.

6.1.6 Boundary conditions

The test set up described in Ala-Outinen (2007) include stiff endplates larger than the cross section welded to each end of the columns to get the support condition as close to fully clamped as possible.

To model the support conditions used in the experiments all degrees of freedom apart from axial translation are locked for the nodes at one end of the columns i.e. the end where the loads are applied. At the other end all degrees of freedom are locked.

To apply the load a reference node is created centrically at one end of the column and the Abaqus/Standard command *coupling is used to uniformly distribute the point load to the nodes at the end of the columns, Figure 6.8.

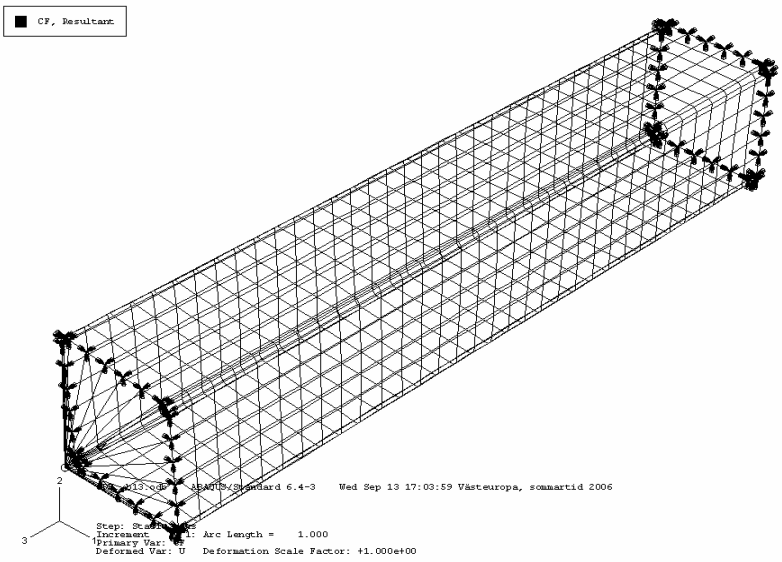

Figure 6.8 ***Applied load and boundary conditions***

6.1.7 Numerical simulation of column tests at room temperature

As a consequence of the sections above the main characteristics of the FE-model are chosen as follows:

- Shell elements, type S4R.
- Average element size, 25 mm.
- Elastic modulus, E=200 000 MPa.
- Poisson's ratio, ν=0,3.

- Non-linear stress-strain curve for the flat faces as the average of performed tensile coupon tests.
- Non-linear stress-strain curve for the corner regions predicted according to Ashraf et al. (2005).
- Corner regions are extended a distance of 2*t* from the curved portions of the cross section.
- Global imperfections, none.
- Local imperfections as the maximum measured imperfection and shape according to eigenvalue analysis.
- Residual stresses, none.
- Boundary conditions, fully clamped at both ends with axial translation released at one end of the column.
- The *Static, Riks analysis in Abaqus/Standard is used to calculate the ultimate compression resistance.

The results of the simulations are compared with the experiments in Table 6.9 below as well as in Figure 6.9 to 6.11.

Table 6.8 ***Compression resistance of columns in room temperature; see Ala-Outinen (2007) for different magnitudes of imperfections***

Section	$N_{u,FEA}$	$N_{u,test}$	$N_{u,FEA}/ N_{u,test}$
150x150x3 (B13)	432 kN	398 kN	1.09
150x150x3 (B16)	430 kN	393 kN	1.09
200x200x5 (A13)	1140 kN	1129 kN	1.01
200x200x5 (A16)	1131 kN	1118 kN	1.01

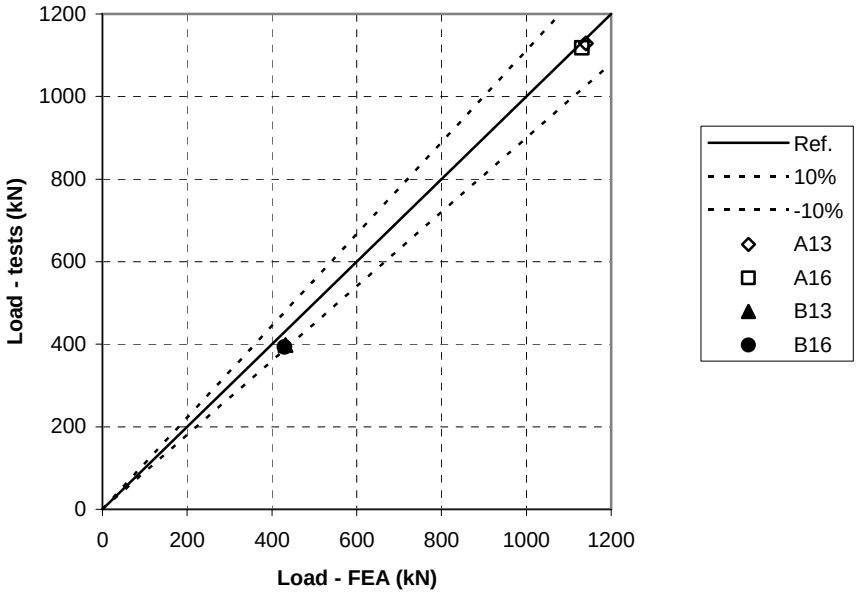

Figure 6.9 ***Comparison of results from FE-model and experiments in room temperature***

Figure 6.10 ***Failure mode experiment***

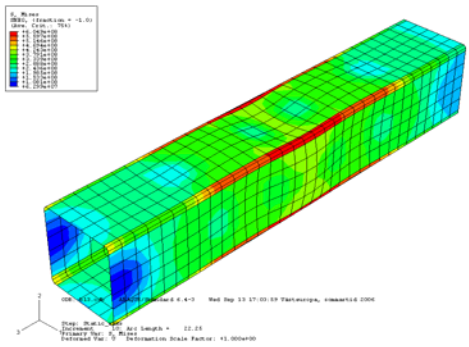

Figure 6.11 ***Failure mode FEA***

It can be seen that the FE-model can calculate the load resistance with good accuracy and that the failure mode i.e. local buckling is consistent with the experiments.

6.1.8 Numerical modelling of column tests at elevated temperature

When measured temperatures of the steel from an experiment are available the easiest way in Abaqus/Standard to make a thermal-dependent static stress analysis is by defining a temperature-time curve and applying it to a field containing a number of elements or nodes. Any thermal dependent material properties can be defined and for instance by applying a thermal expansion coefficient any difference between the initial and applied temperatures will cause a thermal strain.

The temperatures were measured during the tests with twelve chromel-alumel thermocouples, see Ala-Outinen (2007). In the FE-analysis the temperature-time curves from the experiments were approximated with a linear increase in temperature, Figure 6.12. By making sets of elements the possibility to define different temperature-time curves for each one of the thermocouples was obtained. Abaqus/Standard then makes a linear interpolation between the different areas to avoid problems with two different temperatures in the same node. The results obtained by this procedure are that the centre of each set of elements directly relates to the relevant temperature-time curve and the temperature increase between the points are linearly interpolated involving adjacent fields.

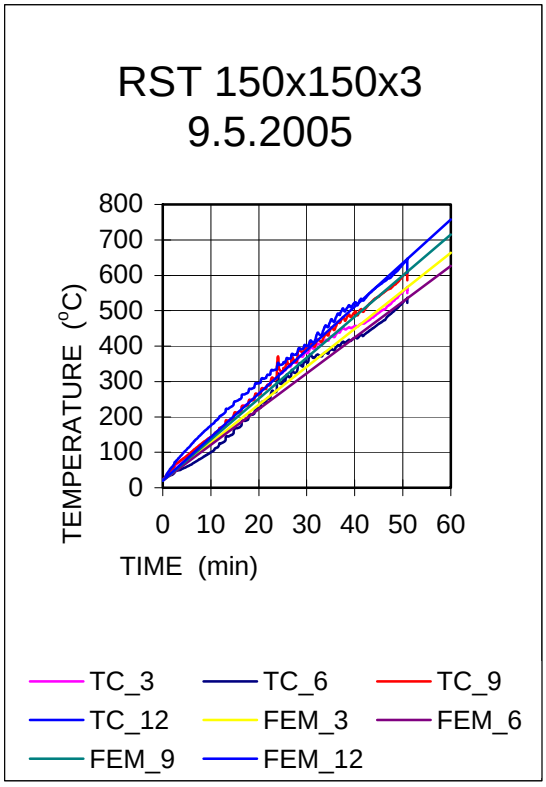

Figure 6.12, ***Example of the approximated linear increase in temperature in the FE-model.***

The main characteristics of the FE-model are taken according to the room temperature analysis with the following differences:

- Temperature dependent Elastic modulus for flat faces, $k_{E,\theta}E$.
- Temperature dependent Elastic modulus for corner regions, $k_{E,\theta,c}E$.
- Non-linear stress-strain curve for the flat faces, $k_{0.2p,\theta}f_{0.2p}$
- Non-linear stress-strain curve for the corner regions, $k_{0.2p,\theta,c}f_{0.2p,c}$
- The thermal expansion coefficient is defined according to EN 1993-1-2 (2005)
- The *Static analysis in Abaqus/Standard is used to calculate the temperature at collapse

The results of the simulations are compared with the experiments in Table 6.10 below as well as in Figure 6.13 to 6.15.

Table 6.9 ***Results from simulations at elevated temperatures; see Ala-Outinen (2007) for different magnitudes of imperfections***

Section		Test				FEA			
	$N_{,fi}$ (kN)	Load level	Temp. (°C)	Exp. (mm)	Time (min)	Temp. (°C)	Exp. (mm)	Time (min)	$Temp_{FEA}/Temp_{Test}$
150x150x3 (B11)	204	0,51	676	7,3	48,3	718	8,8	51,4	1,06
150x150x3 (B14)	165	0,42	720	9,7	55,0	759	10,9	59,1	1,05
150x150x3 (B15)	248	0,63	588	7,1	42,5	595	7,5	43,1	1,01
200x200x5 (A11)	694	0,62	609	-	48,2	482	5,2	37,9	0,79
200x200x5 (A12)	567	0,50	685	8,1	53,3	659	8,0	51,1	0,96
200x200x5 (A15)	463	0,41	764	9,3	57,8	730	9,4	55,8	0,96

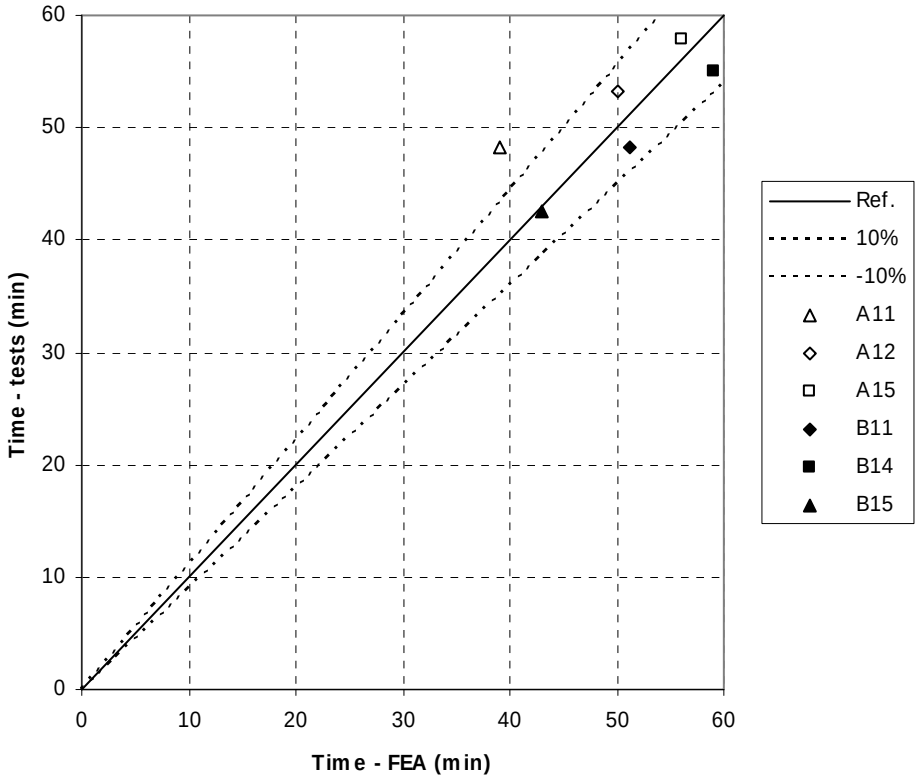

Figure 6.13 ***Failure time, comparison FEA – experiments, specimen number according to Table 6.10***

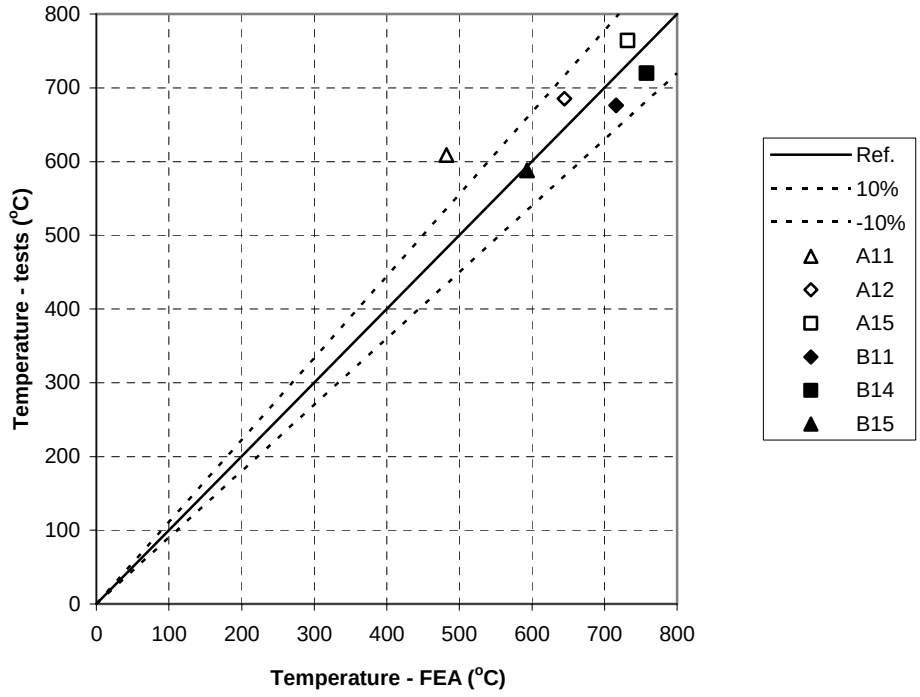

Figure 6.14 ***Failure temperatures, comparison FEA – experiments, specimen number according to Table 6.10***

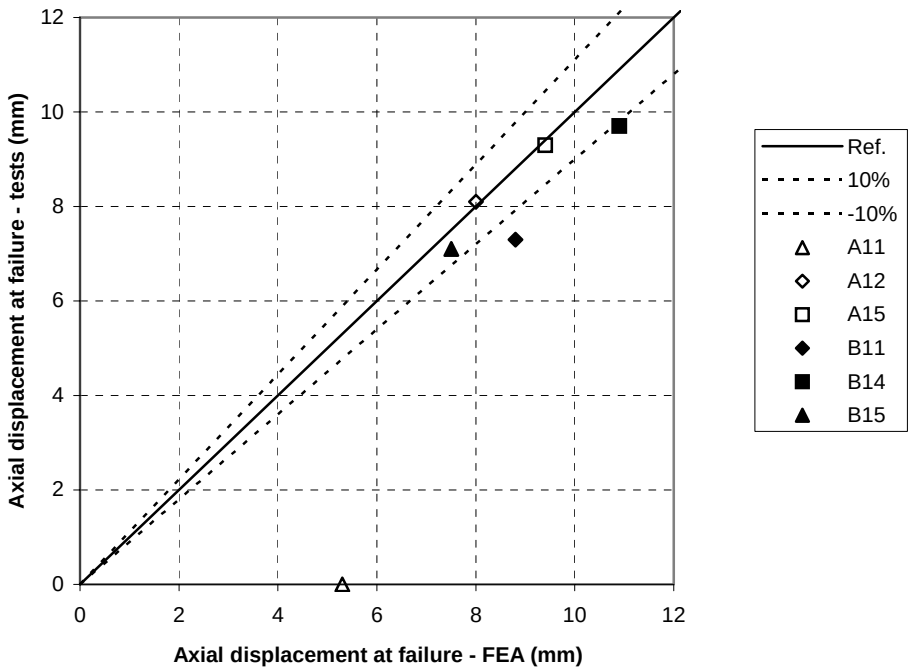

Figure 6.15 ***Displacement at failure, comparison FEA – experiments, specimen number according to Table 6.10***

It can be seen that the FE-model can calculate the failure temperatures with good accuracy for all tests but A11. As a whole the FE-model is considered as acceptable.

6.2 Parametric study

To further investigate the behaviour of thin walled stainless steel box columns a parametric study is performed.

6.2.1 Varied parameters

The following parameters are varied in the parametric study

- Load level: 30%, 40% and 50%
- Cross-section: 100x100x2, 100x100x3, 200x200x4, 200x200x5, 300x300x5 and 300x300x8
- Global slenderness: $\bar{\lambda} = 0,5$, $\bar{\lambda} = 0,8$ and $\bar{\lambda} = 1,2$

All cross-sections are Class 4 but 100x100x3, which is Class 3.
To investigate a possible practical application of class 4 stainless steel columns the parametric study was extended to include the length L=3100mm for all cross-sections and load levels.

6.2.2 FE-model

The validated FE-model described in section 4 was used for the parametric study. However, due to the greater slendernesses simulated than in the experiments the global imperfections has to be taken into account. The local imperfections were taken as b/200 and the global imperfection was taken as L/1000 in accordance with the allowed imperfections in prEN1090-2 (2005). With nominal material properties, including the corner properties, and cross-sectional values the failure loads from the FE-simulations at room temperature were compared to the failure loads calculated in accordance with Design Manual for Structural Stainless Steel (2006), see Figure 6.16. It can be seen that the FE-model gives good agreement with the design method in the Design Manual for Class 4 sections at room temperature. The failure loads from the FE-simulations are then used to calculate the appropriate loads for each load level, cross-section and slenderness used in the simulations at elevated temperatures. The end constraints are pinned for all columns and the temperature distribution are uniform across and along the column.

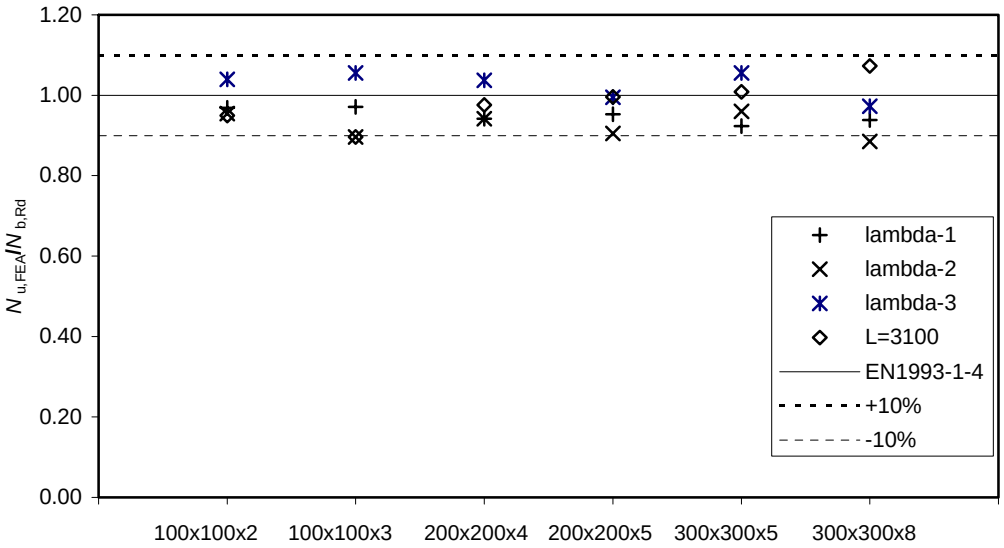

Figure 6.16 ***Comparison of FEA and the design model in Design Manual for Structural Stainless Steel (2006) at ambient temperature***

6.2.3 Results from simulations at ambient temperature

The failure loads at ambient temperature are presented in Table 6.11.

Table 6.11 ***Failure loads for concentrically loaded columns at ambient temperatures***

Specimen-number	Cross-section	Non-dimensional slenderness $\lambda = 0,5$	$\lambda = 0,8$	$\lambda = 1,2$	Length 3100 mm
1	100x100x2	117 kN	89,2 kN	61,9 kN	97,1 kN
2	100x100x3	219 kN	155 kN	116 kN	155 kN
3	200x200x4	457 kN	352 kN	247 kN	502 kN
4	200x200x5	670 kN	494 kN	342 kN	746 kN
5	300x300x5	729 kN	587 kN	408 kN	846 kN
6	300x300x8	1666 kN	1218 kN	846 kN	2030 kN

The results above are used to calculate the different load levels used in the FE-analyses for elevated temperatures.

6.2.4 Results from simulations at elevated temperature

In the FE-analyses the load is kept constant and the temperature is increased step by step.

In order to establish a reliable failure criterion the thermal elongation is compared to the shortening caused by the reduced Elastic modulus. To simplify the calculations the material is assumed to be linear elastic and the strain is calculated at time intervals of 10 °C up to 900 °C. The results give a five times larger strain from thermal elongation than from the reduced Elastic modulus. Even though the material is non-linear and consequently the Elastic modulus at failure probably being smaller than assumed the elongation is believed to be larger than the shortening at all temperature before failure. Hence, the failure temperature is taken as the applied temperature at the moment when the distance between the ends of the column goes from elongation to shortening.

The temperatures at failure from the FE-analyses are presented in Table 6.12.

Table 6.12 ***Temperatures at failure for concentrically loaded columns***

Specimen-number	Cross-section	Load level	Non-dimensional slenderness			Length
			$\lambda = 0,5$	$\lambda = 0,8$	$\lambda = 1,2$	3100 mm
1	100x100x2	30 %	814 °C	840 °C	872 °C	831 °C
		40 %	750 °C	787 °C	825 °C	773 °C
		50 %	678 °C	723 °C	771 °C	707 °C
2	100x100x3	30 %	792 °C	826 °C	862 °C	826 °C
		40 %	720 °C	765 °C	815 °C	765 °C
		50 %	639 °C	696 °C	758 °C	696 °C
3	200x200x4	30 %	814 °C	841 °C	871 °C	810 °C
		40 %	752 °C	788 °C	826 °C	746 °C
		50 %	677 °C	722 °C	785 °C	673 °C
4	200x200x5	30 %	800 °C	830 °C	864 °C	790 °C
		40 %	731 °C	770 °C	816 °C	720 °C
		50 %	652 °C	704 °C	760 °C	643 °C
5	300x300x5	30 %	831 °C	851 °C	881 °C	816 °C
		40 %	771 °C	802 °C	836 °C	750 °C
		50 %	703 °C	740 °C	785 °C	650 °C
6	300x300x8	30 %	800 °C	828 °C	862 °C	780 °C
		40 %	728 °C	768 °C	816 °C	710 °C
		50 %	654 °C	701 °C	758 °C	630 °C

It is seen from the Table 6.12 that the temperature at failure increases with increased global slenderness as well as increased local slenderness. As anticipated the temperatures at failure decreases with higher load levels.

For the length, L=3100 mm and load level 30% the failure temperatures are used to calculate the failure times of the columns when subjected to the Standard fire, ISO 834, by using Equation 6.8. The results are shown in Table 6.13.

$$\Delta\theta_{a,t} = k_{sh} \cdot \frac{A_m/V}{c_a \cdot \rho_a} \cdot \dot{h}_{net,d} \cdot \Delta t \qquad (6.8)$$

where:

k_{sh} is the correction factor for the shadow effect, k_{sh}=1
A_m/V is the section factor for unprotected steel members
A_m is the surface area of the member per unit length
V is the volume of the member per unit length
c_a is the specific heat of steel
Δt is the time interval
ρ_a is the unit mass of steel
$\dot{h}_{net}$ is the design value of the net heat flux per unit area, for the evaluation of $\dot{h}_{net}$ the emissivity, ε_{res}=0,2 and the convection coefficient α_c=35 both in accordance with the Design Manual for Structural Stainless Steel (2006)

Table 6.13 ***Failure temperature from FEA with load level equal to 0.3 and failure times calculated with the standard fire curve (ISO 834)***

Specimen-number	Cross-section	Load level	Length 3100 mm	Failure time (min)
1	100x100x2	30 %	831 °C	29,5
2	100x100x3	30 %	826 °C	30,4
3	200x200x4	30 %	810 °C	28,1
4	200x200x5	30 %	790 °C	27,0
5	300x300x5	30 %	816 °C	30,5
6	300x300x8	30 %	780 °C	30,9

It is clear that it is possible to use unprotected stainless steel columns for fire resistance class R30 if the load level is low.

7. Development of design guidance

7.1 General

The design buckling resistance $N_{b,fi,t,Rd}$ for Class 4 sections is given in Design Manual for Structural Stainless Steel (2006) according to Equation 7.1.

$$N_{b,fi,t,Rd} = \chi_{fi} A_{eff} k_{0.2,p,\theta} f_y / \gamma_{M,fi} \quad (7.1)$$

where: $k_{0.2,p,\theta}$ is the 0,2 % proof strength retention factor at the relevant steel temperature, θ_a.

χ_{fi} is the reduction factor for flexural buckling in fire given by:

$$\chi_{fi} = \frac{1}{\varphi_\theta + \sqrt{\varphi_\theta^2 - \bar{\lambda}_\theta^2}} \text{ but } \chi_{fi} \le 1 \quad (7.2)$$

$$\varphi_\theta = 0,5\left[1 + \alpha\left(\bar{\lambda}_\theta - \bar{\lambda}_0\right) + \bar{\lambda}_\theta\right] \quad (7.3)$$

in which α=0,49 and $\bar{\lambda}_0$ =0,4 for hollow sections.

The modified non-dimensional slenderness $\bar{\lambda}_\theta$ at the steel temperature θ_a is given by:

$$\bar{\lambda}_\theta = \bar{\lambda}\left[\frac{k_{0.2p,\theta}}{k_{E,\theta}}\right]^{0,5} \quad (7.4)$$

where: $\bar{\lambda}$ is the non-dimensional slenderness at ambient temperature and $k_{E,\theta}$ is the retention factor for the slope of the linear elastic range at temperature θ_a.

The design model described above is used to calculate the design buckling resistance at the temperatures at failure from FE-analysis. These are then divided by the applied load from FE-analysis to get the design model's capability to predict the failure loads, Figure 7.1 – 7.3.

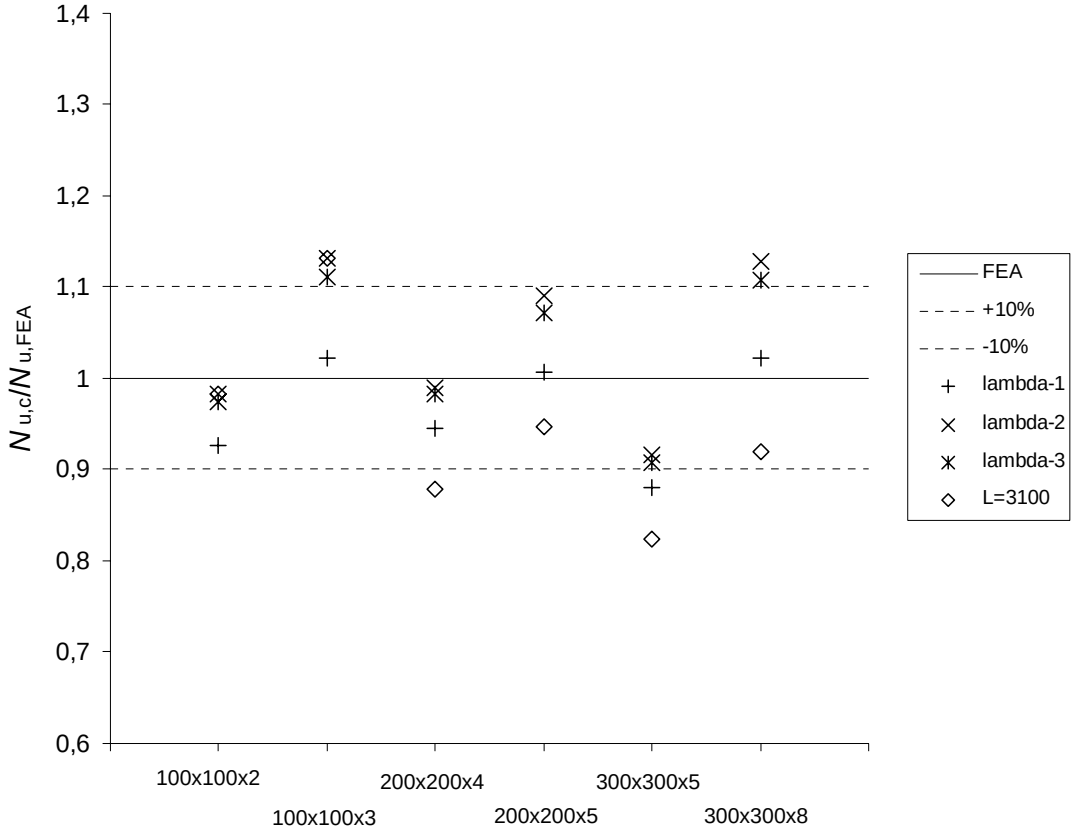

Figure 7.1 ***Comparison of the design model in Design Manual for Structural Stainless Steel (2006) and FEA at elevated temperature, 30 % load level***

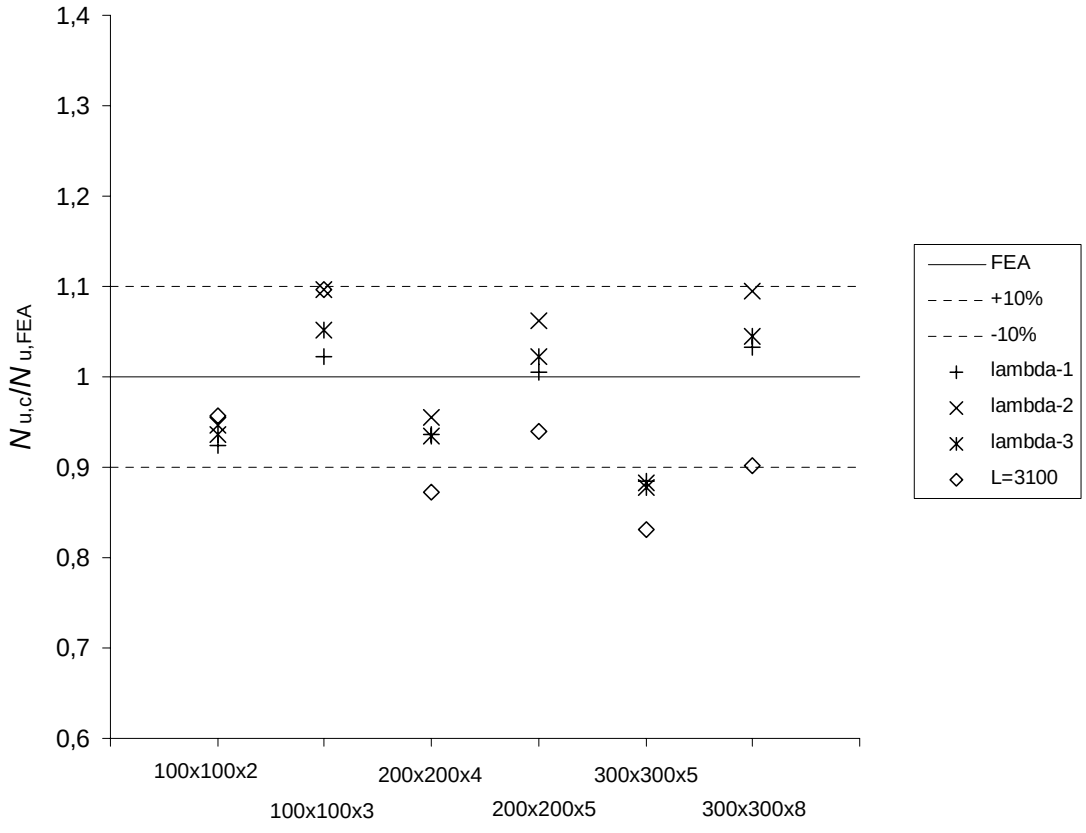

Figure 7.2 ***Comparison of the design model in Design Manual for Structural Stainless Steel (2006) and FEA at elevated temperature, 40 % load level***

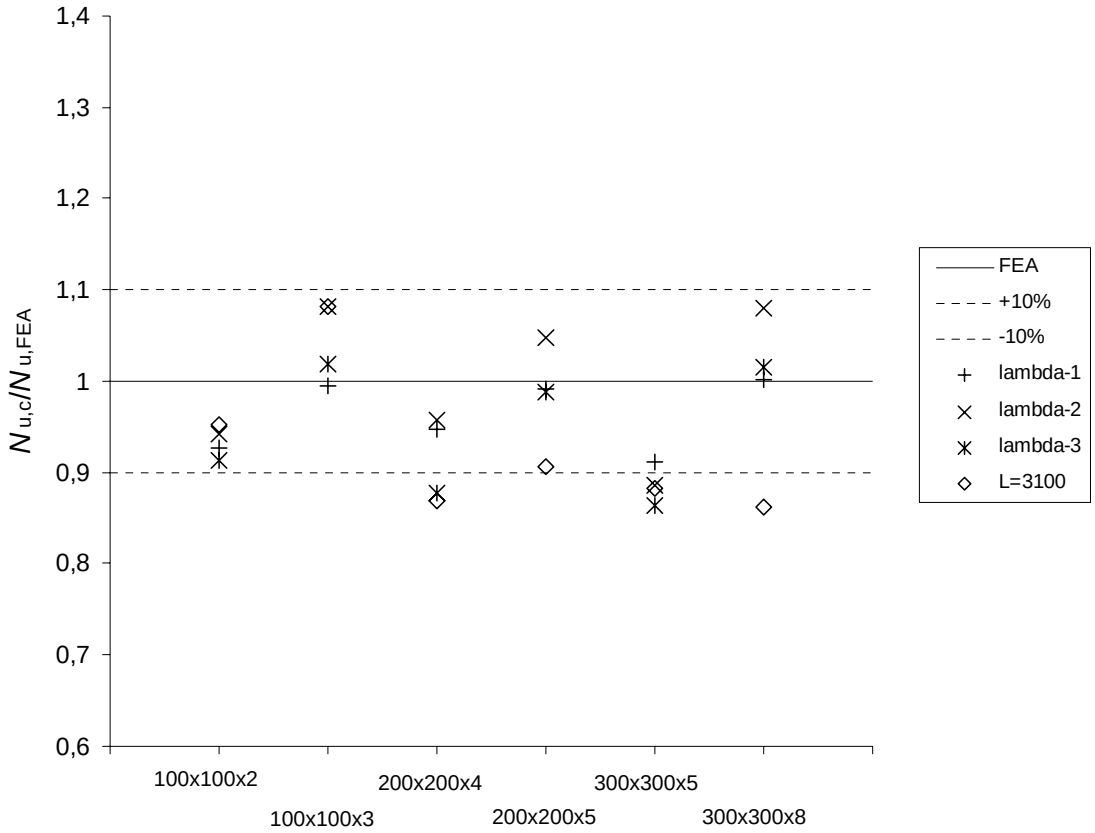

Figure 7.3 ***Comparison of the design model in Design Manual for Structural Stainless Steel (2006) and FEA at elevated temperature, 50 % load level***

It is clear that the design model according to the Design Manual for Structural Stainless Steel (2006) predicts the failure load at elevated temperature with varying accuracy depending on the cross-section slenderness. Greater local slenderness leads to more conservative results. This is a result of the design method neglecting the more favourable relationship between strength and stiffness at elevated temperatures for local buckling.

The intention of the design proposed for elevated temperatures is that it should be valid also for the ambient temperature. Therefore the buckling curve with imperfection factor, α, and the limiting slenderness, $\bar{\lambda}_0$, are taken as 0.49 and 0.4 respectively as it is given in EN 1993-1-4 (2006) as well as in Design Manual of Structural Stainless Steel (2006). The results from the parametric study clearly indicated the importance of taking the temperature dependent relationship between strength and stiffness into account for local buckling as well as for global buckling.

The basic form of the buckling curve given in Design Manual of Structural Stainless Steel (2006), Equation 7.5, is used to further improve the design model.

$$\chi = \frac{1}{\varphi + \left(\varphi^2 - \bar{\lambda}^2\right)^{0.5}} \leq 1 \qquad (7.5a)$$

$$\varphi = 0.5\left[1 + \alpha\left(\bar{\lambda} - \bar{\lambda}_0\right) + \bar{\lambda}^2\right] \qquad (7.5b)$$

Apart from the local and global slenderness being temperature dependent as proposed by Ng & Gardner (2006), Equation 7.6-7.7, the limiting slenderness are suggested to depend on the strength – stiffness ratio according to Equation 7.8.

$$\bar{\lambda}_{p,\theta} = \frac{\bar{b}/t}{28,4\varepsilon_\theta\sqrt{k_\sigma}} \tag{7.6a}$$

where $\bar{b}$ is the relevant width; t is the relevant thickness; and k_σ is the buckling factor.

$$\varepsilon_\theta = \varepsilon\left[\frac{k_{E,\theta}}{k_{0.2p,\theta}}\right]^{0,5} \tag{7.6b}$$

where ε is the material factor; $k_{E,\theta}$ is the reduction factor for Young's modulus; $k_{0.2p,\theta}$ is the reduction factor for 0,2 proof stress.

$$\bar{\lambda}_\theta = \bar{\lambda}\left[\frac{k_{0.2p,\theta}}{k_{E,\theta}}\right]^{0,5} \tag{7.7}$$

$$\bar{\lambda}_{0,\theta} = \bar{\lambda}_0\left[\frac{k_{0.2,p,\theta}}{k_{E,\theta}}\right]^{0,5} \tag{7.8}$$

The proposed design model is given in Equation 7.9 below.

$$N_{b,fi,t,Rd} = \chi_{fi} A_{eff} k_{0,2proof,\theta} f_y/\gamma_{M,fi} \tag{7.9}$$

where:

$$\chi_{fi} = \frac{1}{\varphi_\theta + \sqrt{\varphi_\theta^{\,2} - \bar{\lambda}_\theta^{\,2}}} \text{ but } \chi_{fi} \le 1 \tag{7.10}$$

where: the modified non-dimensional slenderness $\bar{\lambda}_\theta$ at temperature θ is defined in Equation 7.7 and

$\varphi_\theta = 0.5\left[1 + \alpha\left(\bar{\lambda}_\theta - \bar{\lambda}_{0,\theta}\right) + \bar{\lambda}_\theta^{\,2}\right]$

in which α=0,49, for hollow sections according to Design Manual for Structural Stainless Steel (2006) and $\bar{\lambda}_{0,\theta}$, the modified limiting non-dimensional slenderness, is calculated according to Equation 7.8.

The results for the proposed revised design model are given in Figure 7.4 – 7.6.

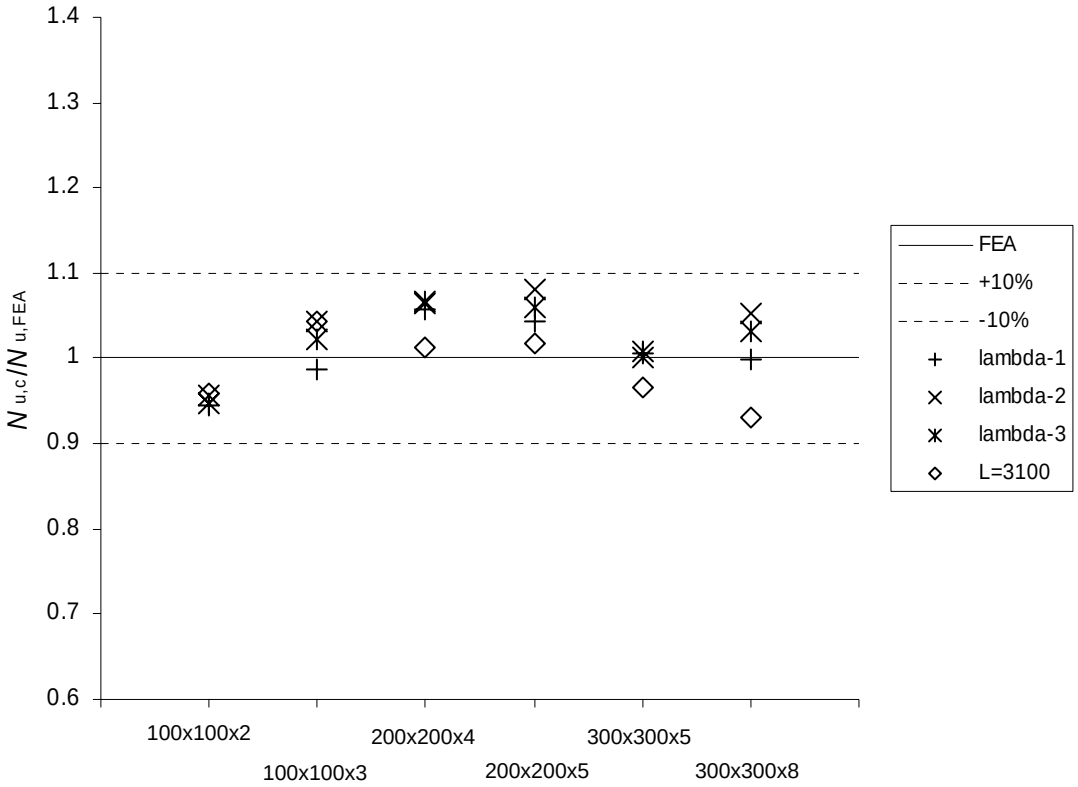

Figure 7.4 ***Comparison of the proposed design model and FEA at elevated temperature, 30 % load level***

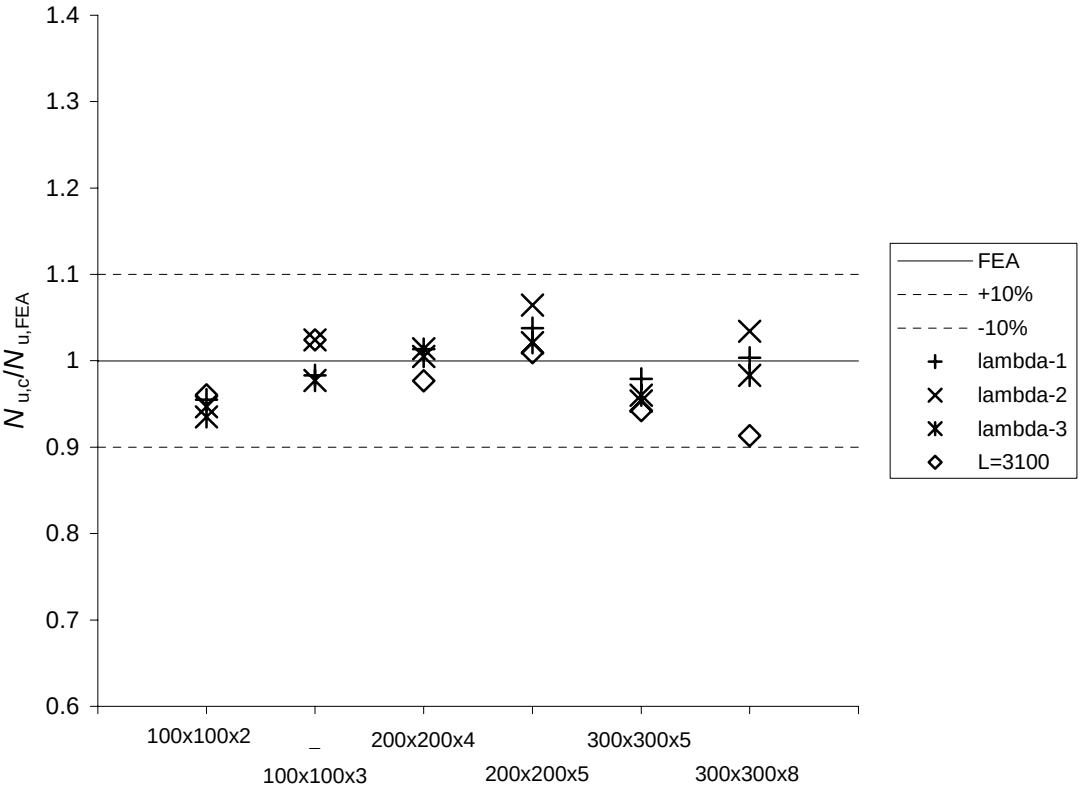

Figure 7.5 ***Comparison of the proposed design model and FEA at elevated temperature, 40 % load level***

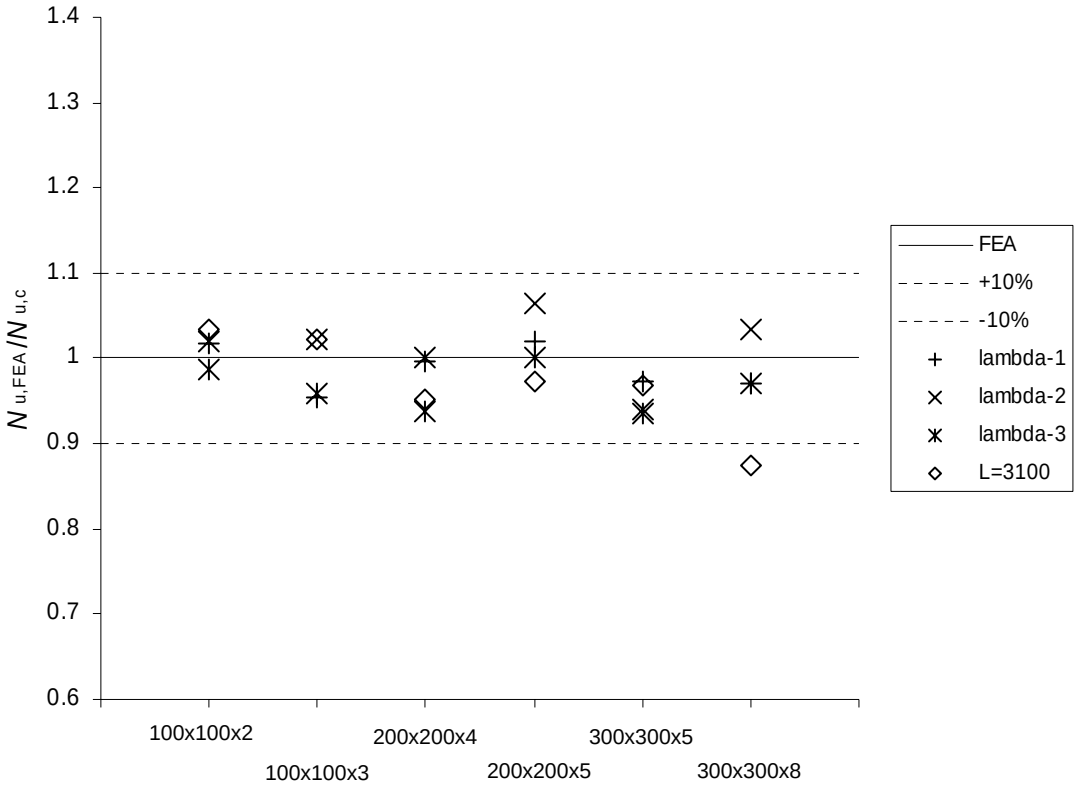

Figure 7.6 ***Comparison of the proposed design model and FEA at elevated temperature, 50 % load level***

A summary of mean values of Design model/FEA and coefficients of variation (COV) are presented in Table 7.1 below. The same for the current design method in EN 1993-1-2 (2005) are also shown.

Table 7.1 ***Mean values and coefficients of variation for different design models for all cross-sections included in the parametric study***

Load level	30 %		40 %		50 %		All load levels	
	Mean	COV	Mean	COV	Mean	COV	Mean	COV
EN 1993-1-2 (2005)	0,78	0,10	0,75	0,10	0,74	0,09	0,75	0,11
Design Manual (2006)	0,99	0,17	0,97	0,14	0,96	0,12	0,97	0,16
Proposal	1,01	0,08	0,99	0,08	0,98	0,11	1,00	0,12

In the parametric study one Class 3 section (100x100x3) was included. In Table 7.2 mean values and coefficients of variation are given for the Class 4 sections included in the parametric study.

Table 7.2 ***Mean values and coefficients of variation for different design models for all Class 4 cross-sections included in the parametric study.***

Load level	30 %		40 %		50 %		All load levels	
	Mean	COV	Mean	COV	Mean	COV	Mean	COV
EN 1993-1-2 (2005)	0,76	0,10	0,74	0,09	0,73	0,08	0,74	0,10
Design Manual (2006)	0,97	0,15	0,95	0,14	0,94	0,14	0,96	0,17
Proposal	1,01	0,08	0,99	0,08	0,98	0,11	0,99	0,12

It is clear that the proposed design model gives improved predictions of the failure loads.

Since the modified limiting non-dimensional slenderness, $\overline{\lambda}_{0,\theta}$ is material dependent as well as temperature dependent eighteen simulations have been made to confirm that the proposed design

model can be used for different stainless steel grades. The simulations were made on cross-sections 200x200x4 and 300x300x5 at 400, 600 and 800 °C with three different global slendernesses, $\bar{\lambda} = 0,5$, $\bar{\lambda} = 0,8$ and $\bar{\lambda} = 1,2$. Another austenitic steel grade, EN 1.4571, was chosen for the analysis. The results are presented in Figure 7.7-7.8.

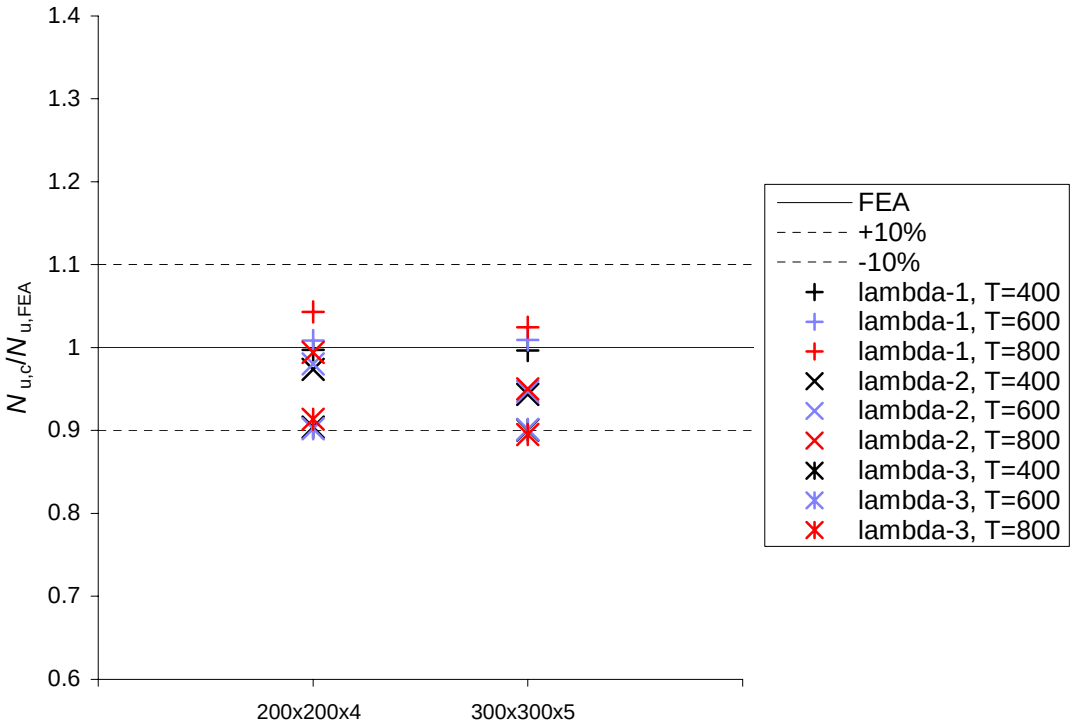

Figure 7.7 ***Comparison of the design model in Design Manual for Structural Stainless Steel (2006) and FEA at elevated temperature, material EN 1.4571***

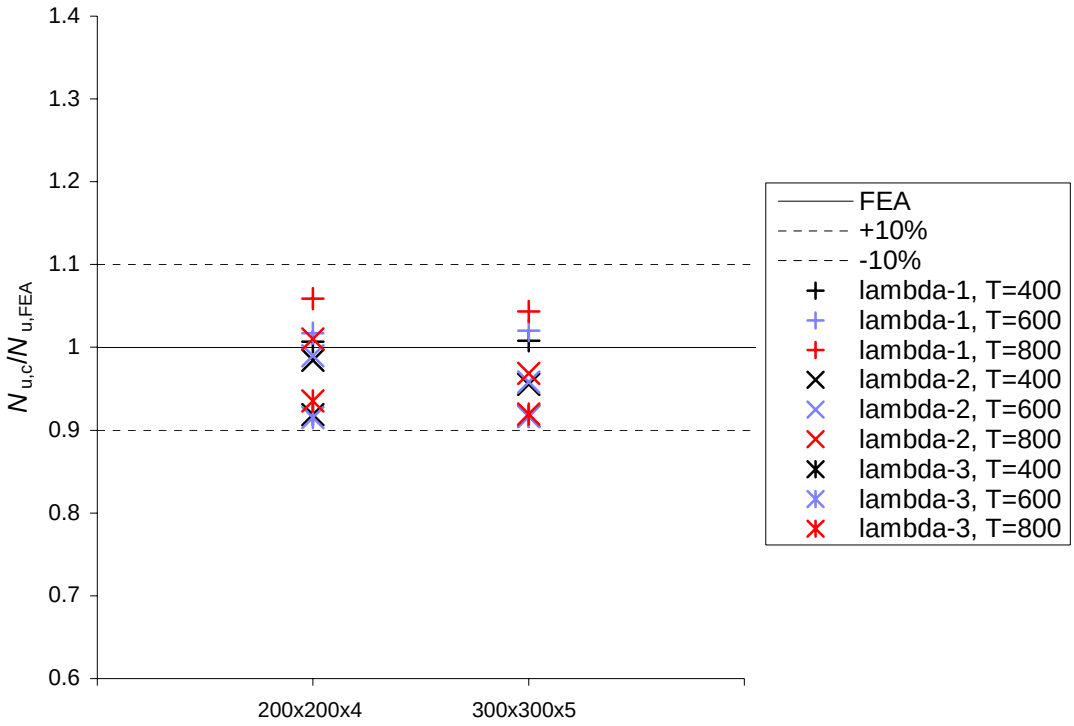

Figure 7.8 ***Comparison of the proposed design model and FEA at elevated temperature, material EN 1.4571***

Although the FE-model has not been validated to column tests with material EN 1.4571 the results indicate that the proposed design also works for different materials. The results give a mean value of Proposed/FEA = 0,97 and COV = 0,08 compared to the Design Manual for Structural Stainless Steel (2006) that give the mean value Design Manual/FEA = 0,96 and COV = 0,08.

8. Conclusions

Design recommendations for Class 4 cross-sections made of austenitic stainless steel presented are fully coherent with EN 1993-1-1 and EN 1993-1-4. This means that:

- the proposed model takes into account better retention of strength and stiffness of stainless steel than carbon steel, and
- the same buckling curve used at ambient temperatures, with $\alpha = 0,49$ and $\overline{\lambda_0} = 0,4$, is used at elevated temperatures.
-

Furthermore, the relationship between strength and stiffness in case of local buckling is taken into account by Equation 7.6.
The proposed design model is consistent with the model for buckling at ambient temperature. The failure loads are predicted with a mean value of 0,99 with the coefficient of variation equal to 0,12 for Class 4 sections. This is an improvement compared to the design model in Design Manual for Structural Stainless Steel where the mean value of the prediction versus test resistance was 0,96 with a coefficient of variation equal to 0,17.

The analysis of 3,1 m long pinned columns in a standard ISO834 fire shows that it is possible to use unprotected Class 4 stainless steel columns and fulfil the requirement for fire resistance class, R30, if the load level is low.

9. Recommendations for further work

Tests on Class 4 members with different stainless steel grades are recommended in order to validate the FE-model and confirm the proposed design model for other materials. It is also proposed to extend the investigations to include eccentricity.

10. References

ABAQUS/Standard manual. 2001. ABAQUS/Standard User's Manual Volumes I-III, Version 6.2. Pawtucket: Hibbitt, Karlsson & Sorenssen, Inc.

Ala-Outinen T. 1996. Fire resistance of austenitic stainless steels Polarit 725 (EN 1.4301) and Polarit 761 (EN 1.4571). *VTT Research Notes 1760.* Espoo: VTT.

Ala-Outinen T. 2007. Tests on Class 4 members in fire. Work Package 3, ECSC project Stainless steel in fire. Contract No. RFS-CR-04048, Espoo: VTT.

Ashraf M. et al. 2005. Strength enhancement of the corner regions of stainless steel cross-sections. In *Journal of constructional steel research*, 61(1): 37-52.

Design Manual for Structural Stainless Steel Third Edition (Building Series, Volume 11). 2006. Euro Inox.

EN 1993-1-1. 2005. Eurocode 3: Design of steel structures – Part 1-1: General rules and rules for buildings, CEN

EN 1993-1-2. 2005. Eurocode 3: Design of steel structures – Part 1.2: General rules – Structural fire design, CEN.

EN 1993-1-4. 2006. Eurocode 3 - Design of steel structures – Part 1-4: General rules – Supplementary rules for stainless steels

Gardner L. & Nethercot D.A. 2004. Numerical modelling of stainless steel structural components – A consistent approach. In *Journal of Structural engineering*, ASCE, 130(10): 1586-1601.

Karlström P. 2004. Thin-walled steel studs in fire: analysis and design recommendations, Licentiat Thesis, Luleå University of Technology, Sweden, 2004:73

Ng K.T. & Gardner L. 2006. Stainless steel compression members in fire. In D. Camotim et al (eds), *Stability and ductility of steel structures. Lisbon, 6-8 Septemper 2006*. London: Imperial College.

prEN 1090-2. 2005. Execution of steel structures and aluminium structures – Part 2: Technical requirements for the execution of steel structures – Stage 34, CEN.

Zhao B. & Blanguernon A. 2004. Member Tests in Fire and Structural Fire Design Guidance. Work package 6, ECSC project Structural design of cold-worked austenitic stainless steel. Contract No 7210-PR-318. London: The Steel Construction Institute.